Multiple time scale dynamics of distance fluctuations in a semiflexible polymer: A one-dimensional generalized Langevin equation treatment

Pallavi Debnath
Department of Inorganic and Physical Chemistry, Indian Institute of Science, Bangalore 560012, India

Wei Min, X. Sunney Xie, and Binny J. Cherayil[a)]
Department of Chemistry and Chemical Biology, Harvard University, Cambridge, Massachusetts 02138

(Received 27 July 2005; accepted 14 September 2005; published online 22 November 2005)

Time-dependent fluctuations in the distance $x(t)$ between two segments along a polymer are one measure of its overall conformational dynamics. The dynamics of $x(t)$, modeled as the coordinate of a particle moving in a one-dimensional potential well in thermal contact with a reservoir, is treated with a generalized Langevin equation whose memory kernel $K(t)$ can be calculated from the time-correlation function of distance fluctuations $C(t) \equiv \langle x(0)x(t) \rangle$. We compute $C(t)$ for a semiflexible continuum model of the polymer and use it to determine $K(t)$ via the GLE. The calculations demonstrate that $C(t)$ is well approximated by a Mittag-Leffler function and $K(t)$ by a power-law decay on time scales of several decades. Both functions depend on a number of parameters characterizing the polymer, including chain length, degree of stiffness, and the number of intervening residues between the two segments. The calculations are compared with the recent observation of a nonexponential $C(t)$ and a power law $K(t)$ in the conformational dynamics within single molecule proteins [Min *et al.*, Phys. Rev. Lett. **94**, 198302 (2005)].
 [DOI: 10.1063/1.2109809]

I. INTRODUCTION

Conformational fluctuations in long chain polymers often occur over a wide range of time scales, ranging from picoseconds (localized side chain rotations) to seconds (collective motions of the backbone). Such fluctuations on multiple time scales lead to highly nonexponential decays for the time-correlation functions of various dynamical properties of the chain.[1,2] In biological systems, similar multiple time scale fluctuations have been implicated in the nonexponentiality of the decay profile of the dynamic structure factor of proteins,[3] as well as in the $1/f^{\alpha}$ noise characterizing ion transport through membrane channels.[4,5] Single-molecule experiments on photoinduced electron transfer between an electron donor and acceptor in the protein complex fluorescein antifluorescein have recently shown that the time-correlation function $C(t)$ of the donor-acceptor distance $x(t)$ also exhibits marked deviations from simple exponential decay.[6,7] In an effort to understand this behavior, Kou and Xie have modeled the dynamics of $x(t)$ by the motion of a fictitious particle in a one-dimensional harmonic well, subject to a random force $F(t)$, and obeying a generalized Langevin equation (GLE).[8] The autocorrelation function of $F(t)$ defines the memory kernel $K(t)$; $K(t)$ in turn is related to the distance correlation function $C(t)$ via the GLE. The experimentally determined $C(t)$ yields a $K(t)$ that can be fit to a power law in time over several decades, with an exponent given by -0.51 ± 0.07.[7] This behavior of $K(t)$ arises when the random force $F(t)$ in the GLE is fractional Gaussian noise.[8,9] However, the molecular basis for the occurrence of such noise in the protein complex is unclear. It remains a challenge to provide a plausible explanation for both the nonexponentiality of $C(t)$ and the power-law decay of $K(t)$, and more generally, to understand anomalous relaxation in complex condensed phase systems.[10] In this paper, as a first attempt, we suggest one possible mechanism for the behavior of $C(t)$ and $K(t)$ using a coarse-grained homopolymer model.

The use of such coarse-grained models to describe the static or dynamic properties of protein molecules with significant secondary and tertiary organizations might be open to question, but recent analyses of protein structures from the Protein Data Bank suggest that proteins have a considerable degree of structural flexibility similar to simple polymers.[11,12] These analyses show, on the one hand, that for a large number of globular proteins, polypeptide segments of more than about 50 amino acid residues *within* the chain behave statistically like random walks,[11] and on the other hand, that *notionally* random coil structures (such as unfolded or denatured proteins) may contain a high percentage of secondary structural elements.[12] Both findings largely corroborate earlier analyses of structural information in protein databases that point to the prevalence of locally and even globally unstructured regions in genomically encoded proteins. Such "natively disordered" regions are distinguished by high conformational flexibility, simple amino acid sequences, and a bias towards certain monomeric residues.[13–15] Their widespread occurrence provides strong evidence for the similarity between proteins and polymers. It is reasonable therefore to seek insights into protein dynamics by studying the dynamics of simple polymers, especially if the dynamics

[a)]Author to whom correspondence should be addressed. Permanent address: Department of Inorganic and Physical Chemistry, Indian Institute of Science, Bangalore 560012, India. Electronic mails: binny@bernstein.harvard.edu, cherayil@ipc.iisc.ernet.in

occur in solution, since the solution phase structures of proteins may be significantly less ordered than their crystal structures.

In this spirit, we conduct the present exploratory study, in which a semiflexible polymer model is used to model the dynamics of protein conformational fluctuations. The predictions of the model are eventually compared to data on distance fluctuations of the fluorescein antifluorescein complex in solution,[7] but the comparison is only intended to be illustrative. Although the crystal structure of the complex is known, the extent to which it resembles the solution phase structure is not, so the model's assumption of the flexible polymer chain is difficult to assess. However, it does produce a nonexponential $C(t)$ and a power-law memory kernel $K(t)$ (in the context of the one-dimensional GLE formalism) that compare favorably with the experimental measurements. Similar models have been used to describe fluorescence resonance energy transfer[16,17] (FRET) and DNA dynamics in laminar flows.[18]

The following section recapitulates the GLE formalism. Section III discusses the semiflexible polymer model, which is defined in terms of a Hamiltonian H, in which a local bending energy is included. The predicted dynamics of $x(t)$ is used to calculate the distance autocorrelation function $C(t)$, and from it, using the one-dimensional GLE approach, the memory kernel $K(t)$. $C(t)$ is found to be well approximated by the Mittag-Leffler function, while $K(t)$ is found to be a power law in time over several decades. The exponent of the power law is studied as a function of chain properties, such as contour length, stiffness, and intersegment separation. The results are discussed in Sec. IV.

II. GENERALIZED LANGEVIN EQUATION AND MEMORY FUNCTION

As stated earlier, the distance fluctuations between two points within a protein, $x(t)$, have been modeled by the GLE for a fictitious particle of mass m in contact with a thermal reservoir at a temperature T, moving under the action of a random force $F(t)$ in a harmonic well U that corresponds to the potential of mean force of the complex. This GLE is given by[7,8,19,20]

$$m\frac{d^2x(t)}{dt^2} = -\zeta\int_0^t dt' K(t-t')\frac{dx(t')}{dt'} - \frac{dU(x)}{dx} + F(t). \quad (1)$$

Here, ζ is the friction coefficient, $K(t)$ is the memory kernel, which is related to the random force $F(t)$ by a generalized fluctuation-dissipation theorem, i.e.,

$$K(t-t') = \frac{1}{\zeta k_B T}\langle F(t)F(t')\rangle, \quad (2)$$

and U is the potential of mean force, which as shown by Min *et al.*[7] can be described by a harmonic well, such that $U = m\omega^2 x^2/2$, with ω a phenomenological frequency that can be extracted from the experimental data on distance fluctuations.

In real polymers, the time evolution of the position $\mathbf{r}_i(t)$ of the ith monomer (in a chain of n monomers) is coupled to the time evolution of the position $\mathbf{r}_j(t)$ of the jth monomer, so $x(t)(\equiv|\mathbf{r}_i(t)-\mathbf{r}_j(t)|)$ is in general a *functional* of the chain conformation, rather than a *function* of $x(t)$ alone, as assumed in Eq. (1). In general, therefore, the GLE for $x(t)$ is not given by Eq. (1), but is instead obtained from the Liouville equation for the complete phase space of the polymer and solvent after the application of projection operators to eliminate the putatively "fast" dynamics of the solvent. This approach, as shown by Schweizer,[21] leads to an equation for the monomer position of the *approximate* form

$$m\frac{\partial^2\mathbf{r}_i(t)}{\partial t^2} = -\frac{1}{k_B T}\int_0^t dt'\sum_{j=1}^{n}\langle\mathbf{F}_i\cdot\mathbf{F}_j^Q(t-t')\rangle\frac{\partial\mathbf{r}_j(t')}{\partial t'} - \frac{\delta W[\mathbf{r}_i(t)]}{\delta\mathbf{r}_i(t)} + \mathbf{F}_i^Q(t). \quad (3)$$

Here W is the n-body intramolecular potential of mean force (a functional of the chain conformation), $\mathbf{F}_i^Q(t)$ is a projected (or "random") force acting at the location of the point $\mathbf{r}_i(t)$ at time t, and $\mathbf{F}_i \equiv \mathbf{F}_i^Q(t=0)$. The time-correlation function of the random force in Eq. (3) is by definition the memory function, which we shall denote $M_{i,j}(t-t')$, and is analogous to Eq. (2) defining $K(t-t')$, but differs from it in having an additional dependence on the segment positions i and j, a reflection of the dynamical coupling between different monomers. In general, $K(t-t')$ is not expected to be the same as $M_{i,j}(t-t')$.

However, the dependence of $M_{i,j}(t-t')$ on i and j makes it extremely difficult to solve Eq. (3) without introducing numerous simplifying approximations.[21] Because such approximations are largely uncontrolled, they can usually be justified only *a posteriori*. Under these circumstances, it is more convenient to work directly with the simplified GLE of Eq. (1) from the outset, and to rely on comparisons of its predictions with experimental results to assess its overall effectiveness. A similar approach is adopted by Russell and Sceats in their study of polymer cyclization kinetics.[22]

With Eq. (1) as a starting point, therefore, we proceed to the evaluation of the memory function. The first step is to simplify Eq. (1) further by assuming conditions of high friction (the overdamped limit), such that the acceleration term may be neglected. This leads to

$$m\omega^2 x(t) = -\zeta\int_0^t dt' K(t-t')\frac{dx(t')}{dt'} + F(t). \quad (4)$$

This equation can be rewritten in terms of the correlation function $C(t)=\langle x(t)x(0)\rangle$ by multiplying it by $x(0)$, and averaging over the equilibrium distribution of initial positions, noting that the correlation function $\langle F(t)x(0)\rangle$ vanishes by virtue of the properties of the random force $F(t)$. In this way, one easily finds that

$$m\omega^2 C(t) = -\zeta\int_0^t dt' K(t-t')\frac{dC(t')}{dt'}. \quad (5)$$

Ordinarily, Eq. (5) would have been used to find $C(t)$ from a proposed expression for $K(t)$. Indeed, if the random force $F(t)$ is assumed to be fractional Gaussian noise,[7,8] $K(t)$ is a power law in t, and $C(t)$ can be calculated from Eq. (5) in closed form in terms of the Mittag-Leffler function $E_\alpha(t)$

[defined by the series expansion $E_\alpha(t)=\Sigma_{k=0}^{\infty}t^k/\Gamma(\alpha k+1)$, where $\Gamma(x)$ is the gamma function]. A satisfactory fit between the experimental $C(t)$ and the function $E_\alpha(t)$ is obtained when $\alpha=1/2$ (at which value the Mittag-Leffler function can be expressed in terms of the error function[7]). Since $F(t)$ is not known in general, however, Eq. (5) is instead inverted so that $K(t)$ is expressed in terms of $C(t)$. This inversion is easily carried out in Laplace space to produce

$$\hat{K}(s)=\frac{m\omega^2}{\zeta}\frac{\hat{C}(s)}{C(0)-s\hat{C}(s)}, \tag{6}$$

where the Laplace transform of a function $g(t)$ is defined by $\hat{g}(s)=\int_0^\infty dtg(t)\exp(-st)$.

The critical next step is the evaluation of $\hat{C}(s)$. In Ref. 7, $\hat{C}(s)$ was obtained from experiment, and substituted into Eq. (6) to produce a $K(t)$ that was found to be a power law in t. In the present calculation, we determine $C(t)$ from a microscopic polymer model, and then obtain the corresponding memory function using Eq. (6). In particular, we fit the calculated $K(t)$ to the experimental data on fluorescein antifluorescein by appropriate choice of the phenomenological parameters in the polymer model.

III. CHAIN DYNAMICS

We model the polymer as a continuous curve, so that a given conformation of the chain is specified by a set of vectors $\{\mathbf{r}(\tau)\}$, which define the spatial coordinates, with respect to an arbitrary origin, of the monomers that are located at the points τ along the chain backbone. The midpoint of the chain is defined to lie at $\tau=0$. The total contour length of the chain is taken to be N, so $-N/2\leqslant\tau\leqslant N/2$. In units where the thermal energy k_BT is defined to be 1, the Hamiltonian H of this model, at the time t, can be written as[23–26]

$$H=\nu\int_{-N/2}^{N/2}d\tau\left|\frac{\partial\mathbf{r}(\tau,t)}{\partial\tau}\right|^2+\frac{\varepsilon}{2}\int_{-N/2}^{N/2}d\tau\left|\frac{\partial\mathbf{u}(\tau,t)}{\partial\tau}\right|^2 + \nu_0(|\mathbf{u}(-N/2,t)|^2+|\mathbf{u}(N/2,t)|^2), \tag{7}$$

where

$$\nu=\frac{3p}{2},\quad \varepsilon=\frac{3}{4p},\quad \nu_0=\frac{3}{4}, \tag{8}$$

and

$$\mathbf{u}(\tau,t)=\frac{\partial\mathbf{r}(\tau,t)}{\partial\tau}. \tag{9}$$

The first term in Eq. (7) describes the connectivity of the chain (which is purely entropic in origin), while the second describes its bending energy; ε and ν are the bending and stretching elastic constants of the chain, respectively, which depend only on the persistence length $L_p\equiv 1/2p$. Nonlocal interactions of the chain segments are not included in H, which is essentially identical to the Hamiltonian used by Cao and co-workers.[16] to investigate fluorescence decay in proteins and polypeptides. But as discussed in the following section, the dynamical equations derived from H are treated exactly, without invoking the Gaussian decomposition approximation used in Ref. 16.

In general, as dictated by differential geometry, the tangent vector $\mathbf{u}(\tau,t)$ must be a unit vector[27] (thus ensuring the inextensibility of the chain) but this constraint is difficult to enforce rigorously, so the requirement of inextensibility is relaxed to the weaker constraint $\langle\mathbf{u}(\tau,t)^2\rangle=1$, where the angular brackets refer to an equilibrium average over the conformations of the chain. This constraint, as shown by Lagowski and Noolandi,[23] is implemented by the inclusion of the last two terms in Eq. (7), and yields a model in which the chain is inextensible only on average.

In the above continuum representation of the chain, the vectorial distance between any two points τ_1 and τ_2 on the chain backbone at the time t is given by

$$\mathbf{d}(t)=\mathbf{r}(\tau_1,t)-\mathbf{r}(\tau_2,t). \tag{10}$$

The absolute value of $\mathbf{d}(t)$ is the dynamical variable of interest, but since magnitudes of vectors are difficult to treat analytically, we shall simply approximate $C(t)$ by the dot product $\langle\mathbf{d}(t)\cdot\mathbf{d}(0)\rangle$. From Eq. (10), this product is given by

$$\langle\mathbf{d}(t)\cdot\mathbf{d}(0)\rangle=\langle\mathbf{r}(\tau_1,t)\cdot\mathbf{r}(\tau_1,0)\rangle-\langle\mathbf{r}(\tau_2,t)\cdot\mathbf{r}(\tau_1,0)\rangle - \langle\mathbf{r}(\tau_1,t)\cdot\mathbf{r}(\tau_2,0)\rangle+\langle\mathbf{r}(\tau_2,t)\cdot\mathbf{r}(\tau_2,0)\rangle \tag{11a}$$

$$\equiv C(t;\tau_1,\tau_2). \tag{11b}$$

As shown in the Appendix, each of the averages on the right-hand side of Eq. (11a) can be calculated from the following general expression:

$$\langle\mathbf{r}(\tau_1,t)\cdot\mathbf{r}(\tau_2,0)\rangle=\sum_{n=0}^{\infty}\int_{-N/2}^{N/2}d\tau Q_n(\tau_1)Q_n(\tau) \times\langle\mathbf{r}(\tau,0)\cdot\mathbf{r}(\tau_2,0)\rangle\exp(-\lambda_n t/\zeta_m). \tag{12}$$

Here Q_n and λ_n are, respectively, the eigenfunctions and eigenvalues of the dynamical equation derived from H [cf. Eq. (A1)]; ζ_m is the monomer friction coefficient and $\langle\mathbf{r}(\tau,0)\cdot\mathbf{r}(\tau_2,0)\rangle$ is an equilibrium correlation function that has been shown to be given by[26]

$$\langle\mathbf{r}(\tau_1,0)\cdot\mathbf{r}(\tau_2,0)\rangle=\frac{\min\{\tau_2,\tau_1\}}{p}-\frac{1}{4p^2}[1-\exp(-2p\tau_2) - \exp(-2p\tau_1)+\exp(-2p|\tau_2-\tau_1|)]. \tag{13}$$

From Eq. (13) and the expressions for Q_n [Eqs. (A10) and (A11)] and λ_n [Eqs. (A14)–(A17)], the integral over τ in Eq. (12) is easily carried out. Eventually, $C(t;\tau_1,\tau_2)$ can be expressed in the form

$$C(t;\tau_1,\tau_2)=\langle\mathbf{d}(t)\cdot\mathbf{d}(0)\rangle_E+\langle\mathbf{d}(t)\cdot\mathbf{d}(0)\rangle_O \tag{14a}$$

$$\equiv C_E(t;\tau_1,\tau_2)+C_O(t;\tau_1,\tau_2), \tag{14b}$$

where $\langle\mathbf{d}(t)\cdot\mathbf{d}(0)\rangle_E$ and $\langle\mathbf{d}(t)\cdot\mathbf{d}(0)\rangle_O$ are the even and odd parity contributions to $\langle\mathbf{d}(t)\cdot\mathbf{d}(0)\rangle$, respectively. The final expressions for these contributions are quite lengthy and are shown in the Appendix [Eqs. (A22) and (A24), respectively].

When calculating the memory function, following the approach described in the previous section, the quantity of interest is actually the Laplace transform of Eq. (14), which is

$$\hat{C}(s;\tau_1,\tau_2) = \hat{C}_E(s;\tau_1,\tau_2) + \hat{C}_O(s;\tau_1,\tau_2). \tag{15}$$

Since the time dependence in Eq. (14) enters solely through the factor of $\exp(-\lambda_n t/\zeta_m)$, the functions $\hat{C}_E(s;\tau_1,\tau_2)$ and $\hat{C}_O(s;\tau_1,\tau_2)$ differ from $C_E(t;\tau_1,\tau_2)$ and $C_O(t;\tau_1,\tau_2)$ [Eqs. (A22) and (A24), respectively] only in the replacement of $\exp(-\lambda_n t/\zeta_m)$ by the factor $1/[s+\lambda_n/\zeta_m]$.

Both $C(t;\tau_1,\tau_2)$ and $K(t)$ are functions not only of τ_1 and τ_2, but also of the contour length N and the persistence length $L_p \equiv 1/2p$. The latter is conveniently expressed in terms of a dimensionless stiffness parameter z, defined as $z = pN = N/2L_p$, which is large ($\gg 1$) for flexible chains (Rouse limit) and small ($\ll 1$) for stiff chains. The evaluation of $C(t;\tau_1,\tau_2)$ and $K(t)$ for definite values of these parameters (N, τ_1, τ_2, and z) is done numerically, as the eigenvalues λ_n must be obtained from a transcendental equation that cannot be solved in closed form. Details of the evaluation of these two functions are discussed in Appendix II.

IV. RESULTS AND CONCLUSIONS

Using Eq. (6) to determine the memory kernel from $\hat{C}(s;\tau_1,\tau_2)$, we find, for a fairly wide range of N, z, and τ_1 and τ_2 values, that $\hat{K}(s)$ is a power law in s over several decades, the exponents varying between about 0.25–0.48 in absolute value. (The highest exponent value, 0.48, and the one closest to the experimentally determined exponent of 0.49 ± 0.07, was obtained for a chain with the following parameters: $N=5000$, $z=5000$, $\tau_1=2500$, and $\tau_2=-2500$.) Chains can apparently be long or short, stiff or flexible, with small or large separations between τ_1 and τ_2, and still produce power-law memory kernels [within the one-dimensional (1D) GLE framework].

Significantly, however, not all choices of N, z, and τ_1 and τ_2 provide satisfactory, *simultaneous* fits of the calculated $\hat{K}(s)$ and $C(t)$ curves to the corresponding experimental curves of Ref. 7. One set of parameter values that does this is $N=500$, $z=5000$, $\tau_1=24$, and $\tau_2=19$, with the monomer friction coefficient ζ_m/k_BT chosen to be $3.18s^{1/2}$ Å^{-2} so as to agree with the value of ζ/k_BT estimated from experiment.[7] The corresponding distance correlation function $C(t;\tau_1,\tau_2)$ [normalized by $C(0;\tau_1,\tau_2)$] is shown in Fig. 1 (full line), along with the experimentally determined correlation function (open circles), and the Mittag-Leffler function of index 1/2 (dashed line). The above parameter values leading to this curve describe a long flexible polymer in which the given pair of segments are close together.

For exactly the same set of parameter values, the s dependence of $\hat{K}(s)$, normalized by the first theoretical data point, is shown in Fig. 2 (full line), along with the experimental data points, normalized by the first experimental data point (open circles), and their estimated error bounds (dashed lines). The slope of the theoretical curve is estimated as -0.43, while the slope of the experimental curve is estimated as -0.49 ± 0.07.[7] Within experimental error, therefore, the calculated and experimental memory kernel exponents coincide. Interestingly, for the same N and z values, essentially the same degree of agreement between theory and experiment is obtained even if τ_1 and τ_2 are varied, *provided* their difference $|\tau_1 - \tau_2|$ is about 5.

We also find that changes to the parameter ζ_m/k_BT shift the position of the $C(t)$ and $\hat{K}(s)$ curves, but do not otherwise change their form. In particular, $\hat{K}(s)$ remains a power law with the same exponent. Since the experimental distance correlation function is well described by the Mittag-Leffler function $E_{1/2}(-(t/t_0)^{1/2})$ it decays on a characteristic time

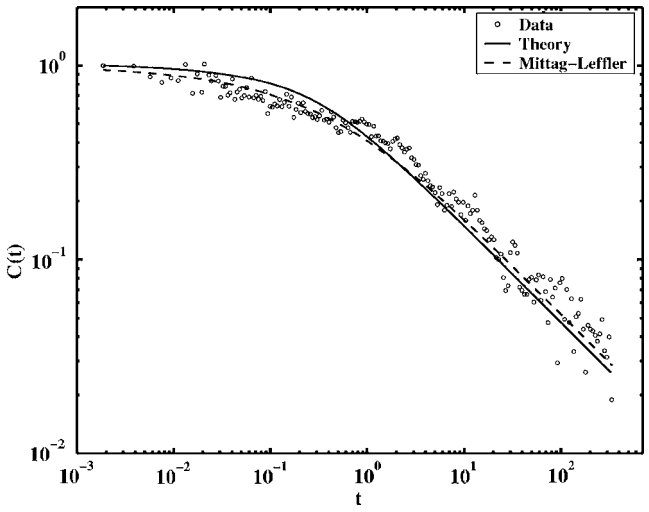

FIG. 1. Distance autocorrelation function $C(t)$ [normalized by $C(0)$] as a function of time t (in seconds). The open circles are the experimental data (normalized by the first experimental data point) on the fluorescein antifluorescein system taken from Ref. 7. The dashed line corresponds to the Mittag-Leffler function of index 1/2, and the full line is obtained from the calculations described in the text. These calculations use the following parameter values: $N=500$, $z=5000$, $\tau_1=24$, $\tau_2=19$, and $\zeta_m/k_BT = 3.18s^{1/2}$ Å^{-2}.

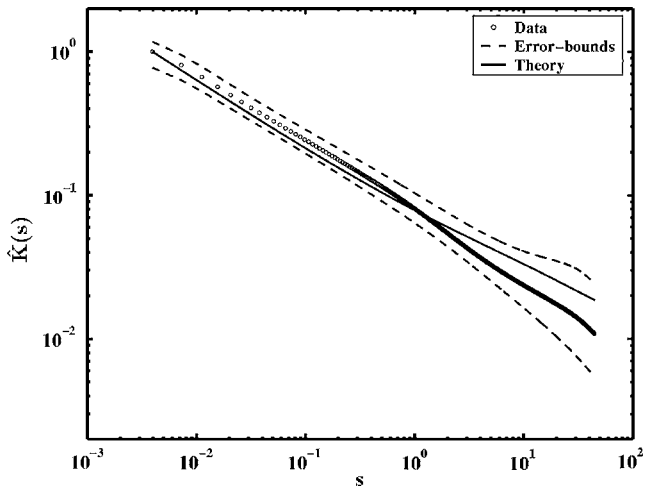

FIG. 2. Memory kernel $\hat{K}(s)$ as a function of s. The open circles are the experimental data points (normalized by the first experimental data point) of Ref. 7. The full line is the theoretical memory kernel (normalized by the first theoretical data point) calculated from the Laplace transform of the $C(t)$ curve shown in Fig. 1 using Eq. (6). The dashed lines correspond to the estimated experimental error bounds.

TABLE I. Memory function exponents $\hat{K}(s) \sim s^b$ in the relation hat for chains of different length N and flexibility z at selected segment positions τ_1 and τ_2.

N	z	τ_1	τ_2	Memory function exponent	Range of power-law decay in s (decades)
500	500	250	−250	−0.41	7
		100	−100	−0.34	7
		50	−50	−0.36	7
500	0.01	250	−250	−0.25	12
		100	−100	−0.25	10
		50	−50	−0.25	11
100	100	50	−50	−0.33	8
		20	−20	−0.29	8
		10	−10	−0.30	9
100	0.01	50	−50	−0.25	12
		20	−20	−0.25	11
		10	−10	−0.25	10
50	50	25	−25	−0.31	8
		10	−10	−0.28	9
		5	−5	−0.27	9
50	0.01	25	−25	−0.25	12
		10	−10	−0.25	10
		5	−5	−0.25	10

scale t_0, which depends on ζ through the relation $t_0 = (m\omega^2/\zeta\Gamma(5/2))^{1/2}$. For the theoretical $C(t)$ to fit the experimental curve, therefore, it must decay on the same time scale t_0. Since this time scale is a nonuniversal quantity that is expected to differ from protein to protein, it is significant that for best fit to both $\hat{K}(s)$ and $C(t)$, the phenomenological parameters of the polymer model cannot be chosen arbitrarily. The ability to discriminate different proteins through t_0 may potentially provide a test of the model's general applicability.

As noted earlier, other choices of N, z, and τ_1 and τ_2 also produce power-law memory kernels. A representative selection of results for such choices is shown in Table I. For each value of the chain length N, two values of the stiffness parameter z have been considered, one value ($z=N$) describing the limit of high flexibility, and the other ($z=0.01$) describing the limit of restricted flexibility. The segment positions τ_1 and τ_2 have been chosen to lie at N/m and $-N/m$, respectively, m being an integer. The last column indicates the range of s, in decades, over which $\hat{K}(s)$ is well characterized by a power law.

Table I reveals a few broad trends, the most noticeable being that the greater the stiffness of the chain, the smaller (in absolute value) the memory function exponent, but the larger the range of power-law behavior. Indeed, this range can extend to as much as 12 decades in s for very stiff chains. A second trend seems to be that a decrease in the separation between τ_1 and τ_2 tends to decrease the magnitude of the memory function exponent, though there are exceptions not listed here. The parameter N seems to have a very negligible effect on the exponents, and the parameter ζ_m/k_BT, as mentioned earlier, only shifts the position of the $C(t)$ and $\hat{K}(s)$ curves.

It should be recalled that these results have been derived for a polymer model in which all long-range nonbonded interactions have been omitted. Including these effects (along the lines of Rouse-Zimm and related models,[1,28,29] for instance) is nontrivial, and unlikely to yield transparent analytic formulas. How they affect the behavior of $C(t;\tau_1,\tau_2)$ and $\hat{K}(s)$ is therefore difficult to predict. As an alternative to exploring such questions analytically, one can instead attempt a thoroughgoing numerical study of $C(t)$ [and from it $\hat{K}(s)$] based on the calculation of normal modes derived from a molecularly realistic protein-solvent potential. A comparison of the two approaches would be very useful in establishing the extent to which coarse-grained polymer models adequately capture the complex dynamics of globular proteins.[11–15]

In summary, we have presented a microscopic polymer model in the framework of the one-dimensional GLE that accounts for multi-time-scale fluctuations of the distance between two segments in the polymer chain. Despite the lack of long-range interactions among different segments, this model provides at least one possible origin for the observed power-law memory kernel in proteins.

Note added in proof: After the submission of our paper, we learned of a related work by R. Granek and J. Klafter [Phys. Rev. Lett. **95**, 098106 (2005)] that uses a fracton model to rationalize power law decays in protein conformational dynamics.

ACKNOWLEDGMENTS

One of the authors (P.D.) is grateful for financial support from the Centre for Scientific and Industrial Research (CSIR), Government of India. Another author (S.X.) acknowledges support from DOE, Office of Science, Office of Basic Energy Science, Chemical Sciences.

APPENDIX A: DYNAMICS OF SEGMENT FLUCTUATIONS

Chain conformations governed by the Hamiltonian H of Eq. (7) evolve in time according to the differential equation[25,26] obtained from the application of Hamilton's principle to the chain Lagrangian $L = 1/2m\int_{-N/2}^{N/2} d\tau |\partial \mathbf{p}(\tau,t)/\partial\tau|^2 - H$, where $\mathbf{p}(\tau,t)$ is the momentum of the monomer at τ at time t. In the limit of large damping, the inertial contribution to this differential equation may be neglected and contributions proportional to the monomer friction coefficient ζ_m and thermal noise added, leading to

$$\left[\zeta_m \frac{\partial}{\partial t} - 2\nu \frac{\partial^2}{\partial \tau^2} + \varepsilon \frac{\partial^4}{\partial \tau^4}\right] \mathbf{r}(\tau,t) = \boldsymbol{\theta}(\tau,t). \tag{A1}$$

This equation must satisfy the following boundary conditions:

$$\left[\varepsilon\frac{\partial^3\mathbf{r}(\tau,t)}{\partial\tau^3}-2\nu\frac{\partial\mathbf{r}(\tau,t)}{\partial\tau}\right]_{\tau=\pm N/2}=0, \tag{A2}$$

$$\left[\varepsilon\frac{\partial^2\mathbf{r}(\tau,t)}{\partial\tau^2}+2\nu_0\frac{\partial\mathbf{r}(\tau,t)}{\partial\tau}\right]_{\tau=+N/2}=0, \tag{A3}$$

$$\left[\varepsilon\frac{\partial^2\mathbf{r}(\tau,t)}{\partial\tau^2}-2\nu_0\frac{\partial\mathbf{r}(\tau,t)}{\partial\tau}\right]_{\tau=-N/2}=0. \tag{A4}$$

Here $\boldsymbol{\theta}(\tau,t)$ is a random force with white-noise statistics that accounts for the effects of thermal noise. From the definition of white noise, we have $\langle\boldsymbol{\theta}(\tau,t)\rangle=0$ and $\langle\theta_\alpha(\tau_1,t_1)\theta_\beta(\tau_2,t_2)\rangle=2\zeta_m^{-1}\delta(\tau_1-\tau_2)\delta(t_1-t_2)\delta_{\alpha\beta}$, where the subscripts α and β refer to the Cartesian components x, y, or z. The solution of Eq. (A1) can be written as[26]

$$\mathbf{r}(\tau,t)=\int_{-N/2}^{N/2}d\tau_1 G_0(\tau,\tau_1|t)\mathbf{r}(\tau_1)+\int_{-N/2}^{N/2}d\tau_1\int_0^t dt_1 G_0(\tau,\tau_1|t-t_1)\boldsymbol{\theta}(\tau_1,t_1), \tag{A5}$$

where G_0 is a Green's function satisfying

$$\left[\zeta_m\frac{\partial}{\partial t}-2\nu\frac{\partial^2}{\partial\tau^2}+\varepsilon\frac{\partial^4}{\partial\tau^4}\right]G_0(\tau,\tau_1|t)=\delta(\tau-\tau_1)\delta(t). \tag{A6}$$

The solution to Eq. (A6) can be expressed as[30]

$$G_0(\tau,\tau_1|t)=\theta(t)\sum_{n=0}^{\infty}Q_n(\tau)Q_n(\tau_1)\exp(-\lambda_n t/\zeta_m), \tag{A7}$$

where $\theta(t)$ is the step function [not to be confused with the random variable introduced in Eq. (A1)], and $Q_n(\tau)$, $n=0,1,2\ldots$, are a complete orthonormal set of eigenfunctions that are the solutions to the following eigenvalue equation:

$$\left[\varepsilon\frac{\partial^4}{\partial\tau^4}-2\nu\frac{\partial^2}{\partial\tau^2}\right]Q_n(\tau)=\lambda_n Q_n(\tau),\quad n=0,1,2,\ldots, \tag{A8}$$

with λ_n the corresponding eigenvalues. The eigenfunctions $Q_n(\tau)$ satisfy the same boundary conditions as defined in Eqs. (A2)–(A4), and can be shown to be given by[25,26]

$$Q_0=\frac{1}{\sqrt{N}}, \tag{A9}$$

$$Q_n(\tau)=\sqrt{\frac{C_n}{N}}\left[-\frac{\cos(\beta_n\tau)}{\sin(\beta_n N/2)}+\frac{\alpha_n\cosh(\alpha_n\tau)}{\beta_n\sinh(\beta_n N/2)}\right]\quad\text{(even parity)}, \tag{A10}$$

$$Q_n(\tau)=\sqrt{\frac{D_n}{N}}\left[\frac{\sin(\beta_n\tau)}{\cos(\beta_n N/2)}+\frac{\alpha_n\sinh(\alpha_n\tau)}{\beta_n\cosh(\beta_n N/2)}\right]\quad\text{(odd parity)}, \tag{A11}$$

where C_n and D_n are normalization constants defined as

$$\left(\frac{C_n}{N}\right)^{-1}=\frac{N}{2}\left(\operatorname{cosec}^2(\beta_n N/2)+\frac{\alpha_n^2}{\beta_n^2}\operatorname{cosech}^2(\alpha_n N/2)\right)+\frac{(\beta_n^2-3\alpha_n^2)}{\beta_n(\alpha_n^2+\beta_n^2)}\left(\cot(\beta_n N/2)+\frac{\alpha_n(\alpha_n^2-3\beta_n^2)}{\beta_n(\beta_n^2-3\alpha_n^2)}\coth(\alpha_n N/2)\right), \tag{A12}$$

$$\left(\frac{D_n}{N}\right)^{-1}=\frac{N}{2}\left(\sec^2(\beta_n N/2)-\frac{\alpha_n^2}{\beta_n^2}\operatorname{sech}^2(\alpha_n N/2)\right)+\frac{(3\alpha_n^2-\beta_n^2)}{\beta_n(\alpha_n^2+\beta_n^2)}\left(\tan(\beta_n N/2)+\frac{\alpha_n(\alpha_n^2-3\beta_n^2)}{\beta_n(3\alpha_n^2-\beta_n^2)}\tanh(\alpha_n N/2)\right). \tag{A13}$$

The parameters α_n and β_n in these expressions are not independent, but are related to each other and to the eigenvalues λ_n by the equations

$$\alpha_n^2-\beta_n^2=\frac{2\nu}{\varepsilon}, \tag{A14}$$

$$\alpha_n^2\beta_n^2=\frac{\lambda_n}{\varepsilon}. \tag{A15}$$

They are obtained from the following equations, which are derived from Eqs. (A2)–(A4) by application of the given boundary conditions, and which correspond to the even and odd parity eigenfunctions found above:

$$\alpha_n^3\cosh(\alpha_n N/2)\sin(\beta_n N/2)+\beta_n^3\cos(\beta_n N/2)\sinh(\alpha_n N/2)+2p(\alpha_n^2+\beta_n^2)\sin(\beta_n N/2)\sinh(\alpha_n N/2)=0\quad\text{(even parity)}, \tag{A16}$$

$$\alpha_n^3\sinh(\alpha_n N/2)\cos(\beta_n N/2)-\beta_n^3\sin(\beta_n N/2)\cosh(\alpha_n N/2)+2p(\alpha_n^2+\beta_n^2)\cos(\beta_n N/2)\cosh(\alpha_n N/2)=0\quad\text{(odd parity)}. \tag{A17}$$

From Eqs. (A5) and (A7), and the property $\langle\boldsymbol{\theta}(\tau,t)\rangle=0$, the correlation function $\langle\mathbf{r}(\tau_1,t)\cdot\mathbf{r}(\tau_2,0)\rangle$ assumes the form [cf. Eq. (12)]

$$\langle\mathbf{r}(\tau_1,t)\cdot\mathbf{r}(\tau_2,0)\rangle=\sum_{n=0}^{\infty}\int_{-N/2}^{N/2}d\tau Q_n(\tau_1)Q_n(\tau)\times\langle\mathbf{r}(\tau,0)\cdot\mathbf{r}(\tau_2,0)\rangle\exp(-\lambda_n t/\zeta_m). \tag{A18}$$

The further evaluation of the monomer time-correlation function in Eq. (A18) requires an expression for $\langle\mathbf{r}(\tau_1,0)\cdot\mathbf{r}(\tau_2,0)\rangle$, which can be shown to be given by[26] [cf. Eq. (13)]

$$\langle \mathbf{r}(\tau_1,0)\cdot\mathbf{r}(\tau_2,0)\rangle = \frac{\min\{\tau_2,\tau_1\}}{p} - \frac{1}{4p^2}[1-\exp(-2p\tau_2) - \exp(-2p\tau_1)+\exp(-2p|\tau_2-\tau_1|)]. \tag{A19}$$

Substituting Eqs. (A9)–(A13) and Eqs. (A18) and (A19) in Eq. (11), and carrying out the integration over τ, we find that

$$C(t;\tau_1,\tau_2) \equiv \langle \mathbf{d}(t)\cdot\mathbf{d}(0)\rangle = \langle \mathbf{d}(t)\cdot\mathbf{d}(0)\rangle_E + \langle \mathbf{d}(t)\cdot\mathbf{d}(0)\rangle_O, \tag{A20}$$

where $\langle \mathbf{d}(t)\cdot\mathbf{d}(0)\rangle_E$ and $\langle \mathbf{d}(t)\cdot\mathbf{d}(0)\rangle_O$ are the even and odd parity contributions to $\langle \mathbf{d}(t)\cdot\mathbf{d}(0)\rangle$, respectively, which are given by

$$\langle \mathbf{d}(t)\cdot\mathbf{d}(0)\rangle_E = \frac{1}{pN}\sum_{\substack{n=2\\ \text{even}}}^{\infty} C_n e^{-\lambda_n t/\zeta_n}(Q_n(\tau_1)-Q_n(\tau_2)) \times\left[\frac{T_1(\tau_2)-T_1(\tau_1)}{\beta_n^2}+\frac{T_2(\tau_1)-T_2(\tau_2)}{\alpha_n^2} + \frac{e^{-pN}}{\alpha_n^2}(\cosh(2p\tau_2)-\cosh(2p\tau_1)) \times\left\{T_2(N/2)+\frac{4p(2p^2+\beta_n^2)}{\beta_n^3}\right\}\right] \tag{A21}$$

$$\equiv C_E(t;\tau_1,\tau_2), \tag{A22}$$

$$\langle \mathbf{d}(t)\cdot\mathbf{d}(0)\rangle_O = \frac{1}{pN}\sum_{\substack{n=1\\ \text{odd}}}^{\infty} D_n e^{-\lambda_n t/\zeta_n}(Q_n(\tau_1)-Q_n(\tau_2)) \times\left[\frac{T_3(\tau_1)-T_3(\tau_2)}{\beta_n^2}+\frac{T_4(\tau_2)-T_4(\tau_1)}{\alpha_n^2} + \frac{e^{-pN}}{\alpha_n^2}(\sinh(2p\tau_1)-\sinh(2p\tau_2)) \times\left\{T_4(N/2)-\frac{4p(2p^2+\beta_n^2)}{\beta_n^3}\right\}\right] \tag{A23}$$

$$\equiv C_O(t;\tau_1,\tau_2). \tag{A24}$$

Here

$$T_1(\tau) = \frac{\cos(\beta_n\tau)}{\sin(\beta_n N/2)} + \frac{\beta_n\cosh(\alpha_n\tau)}{\alpha_n\sinh(\alpha_n N/2)}, \tag{A25}$$

$$T_2(\tau) = \frac{\cos(\beta_n\tau)}{\sin(\beta_n N/2)} + \frac{\alpha_n^3\cosh(\alpha_n\tau)}{\beta_n^3\sinh(\alpha_n N/2)}, \tag{A26}$$

$$T_3(\tau) = \frac{\sin(\beta_n\tau)}{\cos(\beta_n N/2)} - \frac{\beta_n\sinh(\alpha_n\tau)}{\alpha_n\cosh(\alpha_n N/2)}, \tag{A27}$$

$$T_4(\tau) = \frac{\sin(\beta_n\tau)}{\cos(\beta_n N/2)} - \frac{\alpha_n^3\sinh(\alpha_n\tau)}{\beta_n^3\cosh(\alpha_n N/2)}, \tag{A28}$$

and there is no contribution to $\langle \mathbf{d}(t)\cdot\mathbf{d}(0)\rangle$ from the zeroth mode.

APPENDIX B: EVALUATION OF CORRELATION AND MEMORY FUNCTIONS

The evaluation of $C(t;\tau_1,\tau_2)$ [using Eq. (A20) along with Eqs. (A21)–(A28)] and of $\hat{K}(s)$ [using Eq. (6)] can only be done numerically, as the eigenvalues λ_n [which are determined by Eqs. (A14)–(A17)] cannot be obtained in closed form. The calculation proceeds as follows: a definite value is first assigned to the stiffness parameter $z \equiv pN$ by assigning definite values to the contour length N and the parameter p. Variations in z are effected by varying p at constant N or by varying N at constant p. Once z is fixed (thereby also fixing the parameters ν and ε describing the stretching and bending constants, respectively) Eqs. (A16) and (A17) are solved for the parameter α_n, for a chosen value of the mode number n, using Eq. (A14) to express β_n in terms of α_n. The solutions are obtained numerically using Mathematica. The eigenvalue λ_n is then calculated from Eq. (A15), the calculation being then repeated for different n until the complete eigenvalue spectrum is generated. Definite (and arbitrary) values are chosen for the contour positions τ_1 and τ_2, while the parameter ζ_m/k_BT, corresponding to the ratio of the monomer friction coefficient to the thermal energy, is assigned the same value as estimated for ζ/k_BT based on the experimental data. This estimate, in units of $s^{1/2}$ Å^{-2}, is 3.18, and is obtained from these observational findings:[7] $\zeta/m\omega^2 = 0.7 s^{1/2}$ and $k_BT/m\omega^2 = 0.22$ Å^2. The eigenvalues determined above are used in Eqs. (A22) and (A24) along with ζ_m at a prescribed value of the time t to produce definite numerical estimates of $C_E(t;\tau_1,\tau_2)$ and $C_O(t;\tau_1,\tau_2)$, which are added to give $C(t;\tau_1,\tau_2)$. The variable t is then incremented, and the above sequence of steps is repeated to obtain $C_E(t;\tau_1,\tau_2)$, $C_O(t;\tau_1,\tau_2)$, and $C(t;\tau_1,\tau_2)$ at the new value of t. In this way, these quantities are determined as a function of t. We perform the calculation with the first 3184 modes, excluding the zeroth (which drops out of the calculation), obtaining a result that is well converged.

In order to calculate the memory kernel $\hat{K}(s)$ from Eq. (6), a similar procedure is used to first calculate $\hat{C}(s;\tau_1,\tau_2)$, except that in the step involving Eqs. (A22) and (A24), the factor of $\exp(-\lambda_n t/\zeta_m)$ is replaced by the factor $1/[s+\lambda_n/\zeta_m]$. The functions $\hat{C}_E(s;\tau_1,\tau_2)$ and $\hat{C}_O(s;\tau_1,\tau_2)$ are then obtained from these equations at a prescribed value of s (instead of at a prescribed value of t) in exactly the same way as $C_E(t;\tau_1,\tau_2)$ and $C_O(t;\tau_1,\tau_2)$ were obtained earlier. The sum of $\hat{C}_E(s;\tau_1,\tau_2)$ and $\hat{C}_O(s;\tau_1,\tau_2)$ yields $\hat{C}(s;\tau_1,\tau_2)$. After varying s incrementally, and calculating $\hat{C}(s;\tau_1,\tau_2)$ in this way for each new value of the Laplace variable, $\hat{C}(s;\tau_1,\tau_2)$ is eventually obtained as a function of s. This function is now used in Eq. (6) along with $C(0)$ to calculate $\hat{K}(s)$.

[1] M. Doi and S. F. Edwards, *Theory of Polymer Dynamics* (Clarendon, Oxford, 1986).
[2] P.-G. de Gennes, *Scaling Concepts in Polymer Physics* (Cornell University Press, Ithaca, 1979).
[3] G. R. Kneller and K. Hinsen, J. Chem. Phys. **121**, 10278 (2004); G. R. Kneller, Phys. Chem. Chem. Phys. **7**, 2641 (2005).
[4] S. M. Bezrukov and M. Winterhalter, Phys. Rev. Lett. **85**, 202 (2000).
[5] Z. Siwy and A. Fulinski, Phys. Rev. Lett. **89**, 158101 (2002).
[6] H. Yang, G. Luo, P. Karnchanaphanurach, T. M. Louie, I. Rech, S. Cova, L. Y. Xun, and X. S. Xie, Science **302**, 262 (2003).
[7] W. Min, G. Luo, B. J. Cherayil, S. C. Kou, and X. S. Xie, Phys. Rev. Lett. **94**, 198302 (2005).
[8] S. C. Kou and X. S. Xie, Phys. Rev. Lett. **93**, 180603 (2004).
[9] B. Mandelbrot and J. van Ness, SIAM Rev. **10**, 422 (1968).
[10] E. Barkai, Y. Jung, and R. Silbey, Annu. Rev. Phys. Chem. **55**, 457 (2004); R. Metzler, E. Barkai, and J. Klafter, Phys. Rev. Lett. **82**, 3563 (1999).
[11] J. R. Banavar, T. X. Hoang, and A. Maritan, J. Chem. Phys. **122**, 234910 (2005).
[12] N. C. Fitzkee and G. D. Rose, Proc. Natl. Acad. Sci. U.S.A. **101**, 12497 (2004).
[13] P. E. Wright and H. J. Dyson, J. Mol. Biol. **293**, 321 (1999).
[14] S. Vucetic, C. J. Brown, A. K. Dunker, and Z. Obradovic, Proteins: Struct., Funct., Genet. **52**, 573 (2003); A. K. Dunker *et al.*, J. Mol. Graphics Modell. **19**, 26 (2001).
[15] P. H. Weinreb, W. Zhen, A. W. Poon, K. A. Conway, and P. T. Landsbury, Jr., Biochemistry **35**, 13709 (1996).
[16] S. Yang, J. B. Witkoskie, and J. Cao, J. Chem. Phys. **117**, 11010 (2002); S. Yang and J. Cao, *ibid.* **121**, 562 (2004); **121**, 572 (2004).
[17] R. W. Pastor, R. Zwanzig, and A. Szabo, J. Chem. Phys. **105**, 3878 (1996); A. Dua and B. J. Cherayil, *ibid.* **116**, 399 (2002); **117**, 7765 (2002); G. Srinivas, A. Yethiraj, and B. Bagchi, J. Chem. Phys. **114**, 9170 (2001); P. Debnath and B. J. Cherayil, J. Chem. Phys. **120**, 2482 (2004).
[18] A. Dua and B. J. Cherayil, J. Chem. Phys. **112**, 8707 (2000); **113**, 10776 (2000); **119**, 5696 (2003).
[19] D. A. McQuarrie, *Statistical Mechanics* (Harper & Row, New York, 1976).
[20] R. Zwanzig, *Non-Equilibrium Statistical Mechanics* (Oxford University Press, New York, 2001).
[21] K. S. Schweizer, J. Chem. Phys. **91**, 5802 (1989).
[22] W. D. Russell and M. G. Sceats, J. Chem. Phys. **88**, 4526 (1988).
[23] J. B. Lagowski and J. Noolandi, J. Chem. Phys. **95**, 1266 (1991).
[24] M. G. Bawendi and K. F. Freed, J. Chem. Phys. **83**, 2491 (1985).
[25] L. Harnau, R. G. Winkler, and P. Reineker, J. Chem. Phys. **102**, 7750 (1995).
[26] A. Dua and B. J. Cherayil, J. Chem. Phys. **117**, 7765 (2002); **116**, 399 (2002).
[27] K. F. Freed, Adv. Chem. Phys. **22**, 1 (1972).
[28] P. Debnath and B. J. Cherayil, J. Chem. Phys. **120**, 2482 (2004); P. Biswas and B. J. Cherayil, J. Phys. Chem. **99**, 816 (1995).
[29] X. Wang and A. P. Chatterjee, Macromolecules **34**, 1118 (2001).
[30] G. Barton, *Elements of Green's Functions and Propagation: Potentials, Diffusion and Waves* (Oxford University Press, New York, 1989).